Energy calibration and Reconstruction algorithms of the RCS electromagnetic calorimeter

Vahe Mamyan for the RCS collaboration

June 28, 2005

Abstract

To study Real Compton Scattering on the proton an electromagnetic spectrometer was constructed in Hall A at Jefferson Lab. A detailed description of the calorimeter setup and trigger logic is given. The procedures adopted for energy calibration and coordinate reconstructions are discussed. Results of energy and coordinate calibration are presented. The effect of radiation damage on the energy resolution of the calorimeter throughout the experiment is studied.

Contents

1 Introduction

Experiment E99-114 [1] was proposed to measure the cross section of Real Compton Scattering (RCS) at wide range of s and t. A photon spectrometer was designed and constructed to detect the RCS photons. Cornell experiment [2] and calorimeter 25 channel prototype test run [3] provided very valuable information necessary to design the photon spectrometer.

The following are the most important considerations that were taken account while designing the photon spectrometer.

- High energy and angular resolutions.
- Ability to handle high counting rates.
- Veto detector to reject charged particles.

Two planes of veto detectors (vertical and horizontal) were constructed to identify elastic ep electrons. The feasibility studies had shown that the counting rates in the veto were large, so that it was necessary to segment the veto to keep the rate in any given detector less than 500 kHz. The segmentation also allows spatial correlations between hits in the veto and calorimeter. Multihit TDC's were used to improve the veto efficiency at high counting rates.

Energy and angular resolutions were the key features of the photon spectrometer. High energy resolution, better then 10% at half width, was required to separate $ep\gamma$ process from RCS process. High angular resolution was required to estimate the number of photons produced from the decay of π°. The later was the main part of the background present in this experiment. The high angular resolution was obtained by constructing a highly segmented calorimeter (704 channels).

2 Design Consideration

The experiment was going to measure cross section of RCS at 25 different kinematic points. This brought in the requirement to move the photon spectrometer for every kinematic point. A platform was constructed on which the RCS detectors and front-end electronics were mounted. This allowed the platform to be lifted and positioned with the crane to the position at specific predetermined locations on the floor of the hall. The positioning was utilize fiducials on the platform that were aligned with respect to the detectors. The relative location of the calorimeter, veto, was known to a few mm. The required alignment precision was not great (few mm in all dimensions), because of possibility to do calibration on elastic electron scattering events. The Front-end electronics of the Calorimeter was cooled down by high power air blower. The cooling was especially important for dividers. The flexibility of the calorimeter design allowed to replace malfunctioning PMT's within time of one hour. Several PMT's were replaced during the experiment.

3 Lead Glass Array

The calorimeter was made up of a total of 704 lead-glass blocks, with a FEU-84/3 PMT optically coupled to the rear of each block. The lead-glass was arranged in 22 columns and 32 rows, as shown in Fig. 1, leading to a cross-sectional area of 128×88 cm^2. It is housed within a light-proof containment structure with interlocked doors at the rear for easy access to the PMT's. Diagram of the RCS calorimeter which shows the arrangement of the lead-glass blocks, the forced-air cooling system and the cabling, within the calorimeter frame. The lead-glass properties are shown in Tb. 1,

Density ρ	3.86 g/cm^3
Refractive Index n	1.65
Radiation Length X_o	2.5 cm
Moliere Radius R_M	3.3 cm
Critical Energy ϵ_o	15 MeV

Table 1: Properties of TF-1 lead-glass.

The individual blocks had dimensions 4×4×40 cm^3. They were wrapped in aluminized Mylar film and black Tedlar to ensure there was no exposure to external light, which could seriously damage the PMT's. Individual tubes were coupled to the lead-glass by optical grease and pressed into contact by springs attached between a grid of steel supports and the base of the tube. Proper operation of the tube requires reasonably high voltage gradients between dynodes, and in the present case a total voltage difference of 1600 V was applied. The electrical output from each tube is sent to trigger logic and a Fastbus 1881 Analogue-to-Digital Converter (ADC). A gain monitoring system was designed for calibration of the multiple high voltage channels supplying the calorimeter. To expose each PMT to approximately equal light levels, pulsed ultra-violet light from a nitrogen laser was incident on a plastic scintillator, acting as a wavelength shifter and removing the directionality of the laser light, the output from which was then transported in a series of optical fibers to a plate of the transparent plastic lucite. The calorimeter was illuminated by the light from this plate, which was located immediately adjacent to the calorimeter face, spanning its full cross sectional area. The process was fully automated, and operated remotely using Java control software and a LeCroy-1458 based high voltage system.

A support structure was designed to accommodate the calorimeter, the accompanying front-end electronics, the gain monitoring system, the forced-air PMT-base cooling system and the large amount of cables. It also facilitated movement of the entire assembly between the various kinematic points. Also for ease of movement the signal and high voltage cables (over two thousand of them) were placed on a series of bogies at the rear of the calorimeter platform. Finally, small light sources at the front and rear of the support platform shining vertically onto the hall floor were used to align

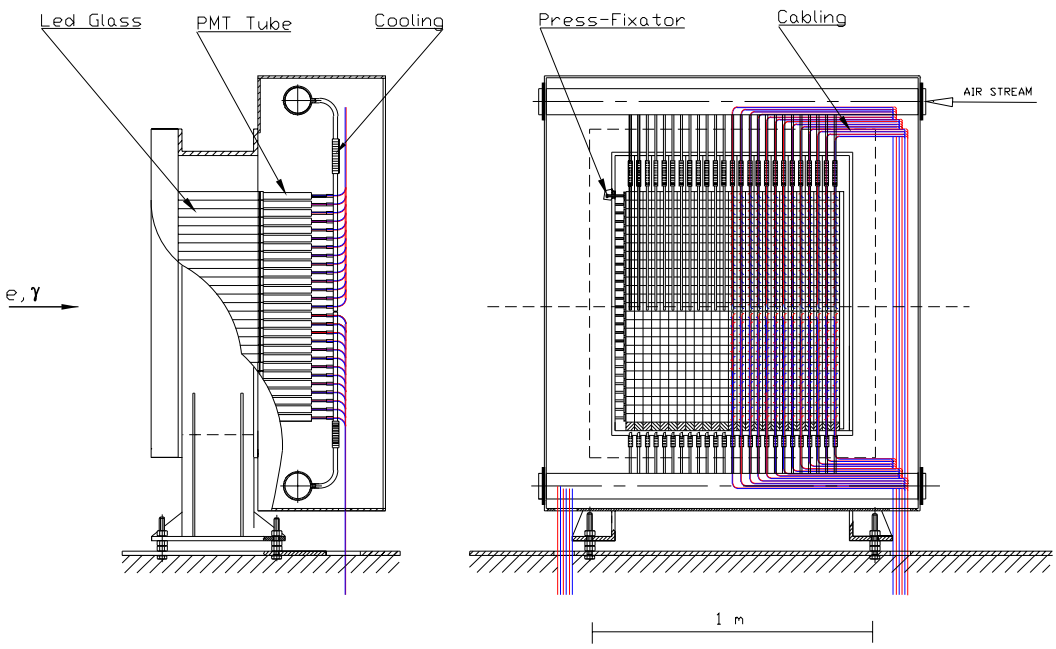

Figure 1: Diagram of the RCS calorimeter which shows the arrangement of the lead-glass blocks, the forced-air cooling system and the cabling, within the calorimeter frame.

the photon-arm to marks painted on the floor. The accuracy of the positioning of the calorimeter was checked by using elastic *ep* data taken before each kinematic point. The difference between expected and measured electron hit position was the criteria (in ideal case it should be centered on zero) being used to judge about the absolute positioning of the calorimeter. The position of the calorimeter was adjusted if there were offsets exceeding calorimeter's coordinate resolution. The marks for each kinematic point, produced by a survey of the experimental hall, provided the desired accuracy while allowing a simple and flexible method for positioning of the spectrometer.

4 Lucite Čerenkov Array

Veto detector was designed to reject high energy electrons. It had two detector

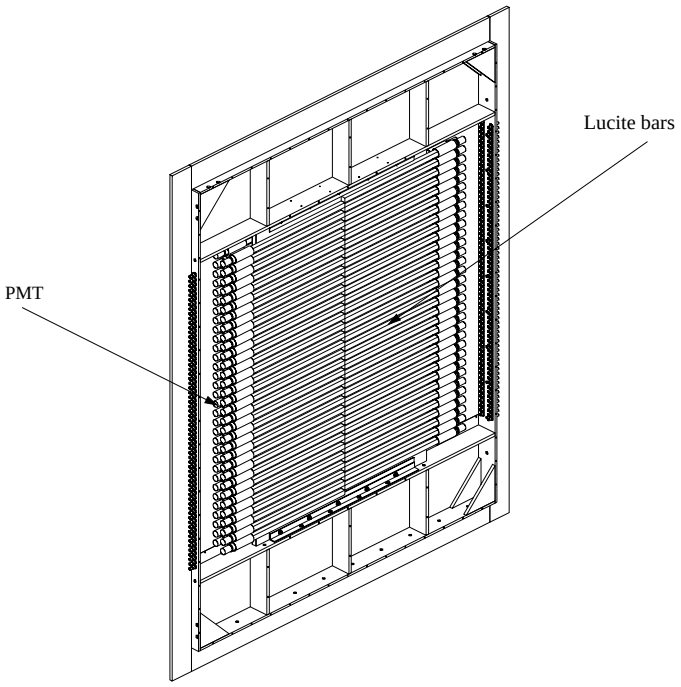

Figure 2: Horizontal Veto plane.

planes called Horizontal Veto (HV) (Fig. 2) and Vertical Veto (VV). The Horizontal and Vertical vetoes were placed in front of the calorimeter at 27.6 cm and 28.7 cm about the front face of the calorimeter, respectively. The HV plane consist of lucite bars each with size 2×2×44 cm, the VV consist of lucite bars each with size 2×2×64 cm. They were wrapped in aluminized Mylar film and black Tedlar to ensure there was no

exposure to external light. The HV had 64×2 bars, the VV has 2×44 bars. Total area covered by the veto detectors was 88×128 cm^2. The principle of electron rejection of veto is that the veto detector produces light flashes as a result of a electron passing through and producing Čerenkov light in it, while neutral particles does not. To each lucite bar a 29 mm diameter PMT was attached by gluing. The PMT model XP2972 with addition amplifier in HV base was used [4].

5 Trigger scheme

The calorimeter trigger was provided by the PMT signals from individual electromagnetic calorimeter blocks, which were summed as shown in Fig. 3. The electrical signals from each of the 2×4 sub-arrays of adjacent lead-glass blocks, excluding the outermost layer, are summed in a linear-summing module to give a sum_8 signal. These, in turn, are further summed in overlapping groups of four to give a sum_{32} signal, of which there are 56 in total. The sum_{32} signals are sent to discriminators which produce

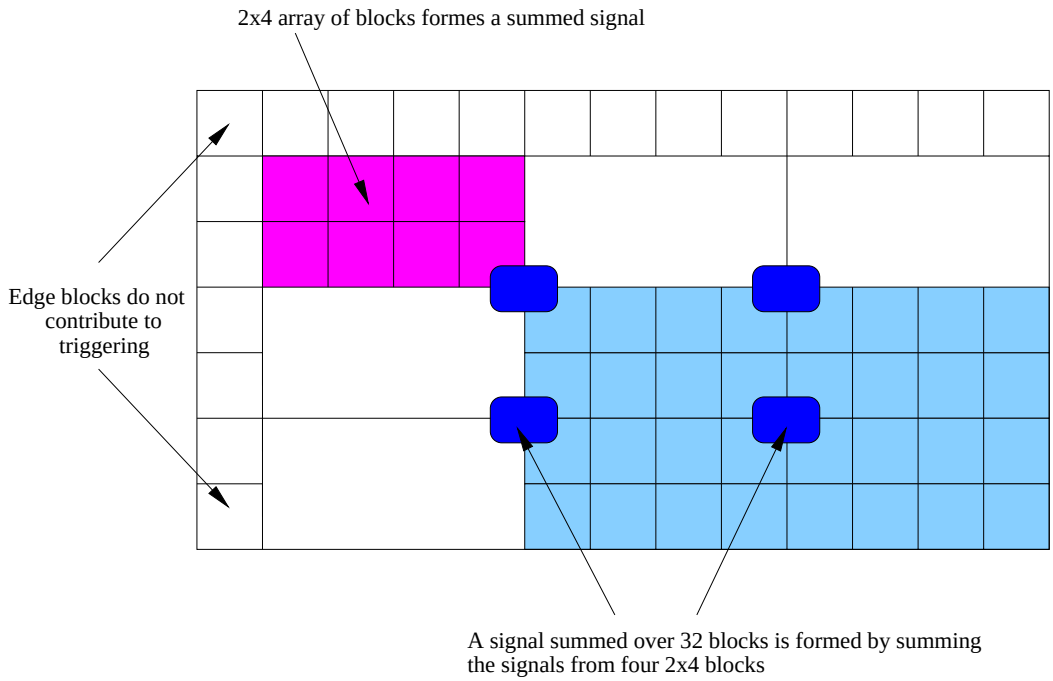

Figure 3: The photon trigger was made up of the OR of 56 overlapped sum_{32} signals, which are firmed by summing signals from adjacent calorimeter blocks.

a logic pulse if the input signal is above a given threshold. The calorimeter singles trigger (T1), formed by taking the logical OR of the sum_{32} signals, was produced only when the total energy accumulated in the calorimeter was above a certain value. The

minimum threshold was set 300 MeV, it was changed proportional to the expected energy of RCS photons, see Fig 4.

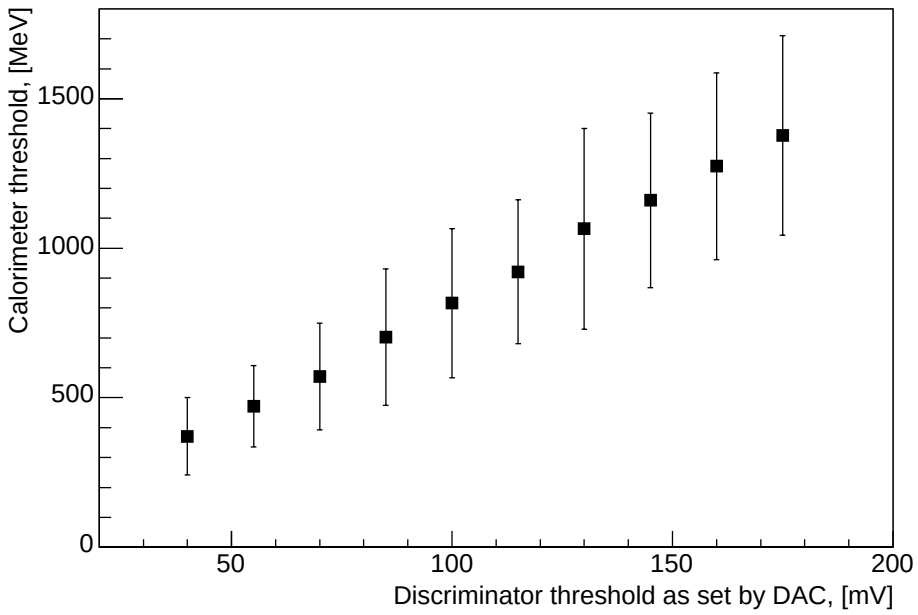

Figure 4: Calorimeter threshold versus discriminator threshold.

The threshold on the calorimeter discriminators (controlled by a single DAC) was calibrated by doing a series of short runs (each approx. 15 minutes) with the T1 trigger (calorimeter singles) and with the threshold changed to see how the energy threshold depends on the electronic threshold. In order for this to be effective, it is necessary for the gains to be well matched so that the electronic threshold is approximately the same energy threshold for each of the 56 discriminators. The error bars in Fig. 4 are reflecting the variations of the signal entering into discriminator. The effect is caused by the form fluctuation of the signal of the electromagnetic shower.

6 Calibration cosmic/beam

To reconstruct the energy deposited in the calorimeter it is necessary to know the coefficients which transform ADC values of each individual block to energy deposited in that very block. The calibration coefficients can be found by detecting particles with known energy. There are other methods to obtain calibration coefficients (cosmic and laser calibrations), but they can not provide the required precision.

- Laser calibration

  The gain drifts happening between calibrations was monitored using the gain monitoring system, providing an accuracy of relative gain measurements of about 0.3%. The system includes a stable light source and a system to distribute the light to all the calorimeter and veto modules. The light source consists of a LN300 nitrogen laser and a wave length shifter. The LN300 laser provides 5 ns long, 300 μJ ultra-violet light pulses of 337 nm wave length. The light passes through absorbers, including a remotely controlled wheel with several calibrated absorbers, lenses, and arrives at a wave length shifter. The wave length shifter used was a semi-spherical piece of plastic scintillator, in which the ultra-violet light was fully absorbed and converted to a blue (425 nm) light pulse, radiated isotropically. Around the scintillator semi-sphere about 40 plastic fibers 2 mm thick were arranged, transporting the light to the veto counter and the photon calorimeter. The light reaches each veto counter via a system of fibers and light splitters, while for the calorimeter a different technique was used. A lucite plate was mounted adjacent to the frontal face of the lead glass calorimeter, covering all the aperture of the calorimeter. The front faces of the glass modules were opened to light. The fibers transport the light from the laser to the side faces of the lucite plate. The light passes through the length of the plate and due to light scattering in lucite the plate slightly glows. This glowing was seen by the lead glass calorimeter modules. Such a system provides a rather uniform light collection for all the modules. The system had been assembled and tested with about 30 calorimeter channels powered up at different locations of the calorimeter matrix. The laser provided enough light - at least 2 orders of magnitude more than needed. The amplitude variance of the signals was about 1% on a pulse-to-pulse basis. The amplitudes of the signals were dropping with time by about 2.5% per day at 1 Hz repetition rate of the laser. Such a drop was about one order of magnitude larger than expected from the specifications of the laser. The most probable explanation was degrading of the plastic scintillator caused by UV light. We monitored the light flash from the scintillator using semiconductor photodiodes which produce a vary stable and linear output.

- Cosmic calibration

  Cosmic calibration was performed for preliminary calibration of the calorimeter. It was used for preliminary adjustment of the PMT gains.

- Beam calibration

  Elastic *ep* data were taken for calorimeter calibration. The energy calibration was performed for every kinematic point where the expected energy of RCS photons was significantly different from that of preceding kinematic point. The energy of

electrons was calculated from the High Resolution Spectrometer assuming two body kinematic. This provided energy calibration scale to better than 1%.

The purpose of the shower cluster reconstruction in a calorimeter is to calculate energy and position of the particle, giving electromagnetic shower in the detector. For this, at first shower cluster is detached. Cluster in a shower detector is determined as a group of adjacent blocks, where electromagnetic shower has been developed, i.e. an energy deposition was detected. Central block of the cluster is defined as the one that has maximum energy deposition. Then parameters of the shower — energy and coordinates — are calculated. Energy E is calculated as sum of energy depositions in all of counters included into the cluster by formula

$$E = \sum_{i \in M} E_i \tag{1}$$

and X, Y coordinates of the cluster are calculated as coordinates of the center of gravity by formulas

$$X = \sum_{i \in M} E_i \cdot X_i / E \ , \qquad Y = \sum_{i \in M} E_i \cdot Y_i / E \tag{2}$$

where:

i	—	number of shower counter, included into the cluster
M	—	set of counters numbers, included into the cluster
E_i	—	energy deposition in the i-th counter
X_i	—	X coordinate of center of the i-th counter
Y_i	—	Y coordinate of center of the i-th counter

Shower counters gain calibration is required to reconstruct parameters of the shower, coordinates and deposited energy. Purpose of calibration is to define a coefficient for transformation of the ADC amplitude to the energy deposition for every shower counter. I.e., define coefficients C_i such that

$$E_i = C_i \cdot (A_i - P_i) \tag{3}$$

where:

A_i	—	ADC amplitude
P_i	—	pedestal of amplitude
C_i	—	calibration coefficient
E_i	—	energy deposition in the i-th counter

The calibration coefficients C_i are calculated by minimization of functional

$$\chi^2 = \sum_{n=1}^{N} \Big[\sum_{i \in M^n} C_i \cdot (A_i^n - P_i) - E_e^n \Big]^2 \tag{4}$$

Here:

$n = 1 \div N$ — Number of event;

i — Number of counter, included into the cluster
M^n — Set of counters numbers in the cluster
A_i^n — Amplitude in the i-th counter
P_i — Pedestal of the i-th channel
E_e^n — Known energy of a particle
C_i — Shower counters calibration coefficients to be fitted

Having the calculated calibration coefficients, energy deposition E, coordinates X, Y of the shower center are calculated by the formulas (1) and (2).

The shower cluster reconstruction algorithm described above had been realized for the RCS gamma calorimeter in the RCS **Analyzer**, which was developed on basis of Hall A C++/ROOT **Analyzer**.

Reconstruction of shower cluster parameters in the calorimeter (as well as database parameters settings, row data decoding, particle identifier setting, etc.), is performed by different functions of the **THaCalorimeter** class.

7 Experimental results

7.1 Calibration Procedure

Elastic *ep* data were taken to calibrate the calorimeter. The following rearrangements were done in the experimental setup before taking the data:

- Position photon spectrometer and HRS to elastic kinematic.
- Remove the radiator that was used to produce the bremsstrahlung photon beam.
- Turn off the deflection magnet of the photon spectrometer.

It was very important to have very clean *ep* elastic events. This implied a condition to run under low current to avoid from the background events that could not be removed by kinematic cuts. We usually ran up to 10μA current, except for a few cases where it was necessary to test calorimeter's performance under high beam current(40μA). At least twenty elastic events in each block was required to include the block into calibration procedure. Otherwise, the block was excluded and the calibration coefficient of that block was fixed and set the one found from the previous calibration. To demonstrate the cleanness of elastic events an example of an *ep* event is shown in Fig. 5. The significance of the plot is the absence of any type of background events. The cluster size used in the calibration and reconstruction procedure was 3×3. Calorimeter counters gain calibration is performed by the stand-alone program. At first, calibration events

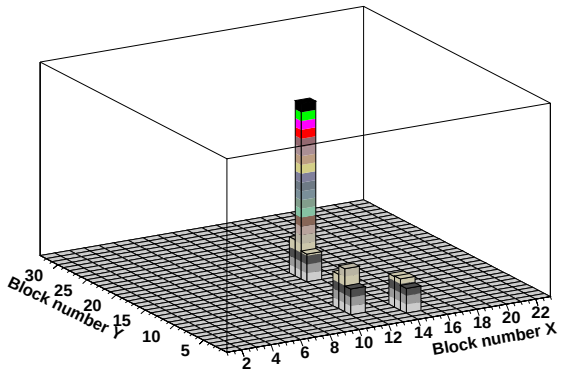

Figure 5: Elastic ep event sample in calorimeter, beam current is 10μA.

are selected (on different conditions — coincidence, particle ID, multiplicity of shower cluster, etc.) by using the output Tree file of the **Analyzer**. Then, calibration coefficients are calculated by minimization of functional (4). Finally, different histograms of reconstructed parameters distribution are plotted.

Also, calibration coefficients values were used to obtain differences between gains of the calorimeter counters. These relative gains are used to equalize ADC amplitudes from the channels by changing HV settings on the counters PMT's.

7.2 Energy and position resolution results

An example of elastic calibration is illustrated in this paragraph. The kinematic settings are shown in Tb. 2.

E beam(GeV)	E calo(GeV)	D calo(m)	θ calo	θ HRS	HRS p(GeV)
5.759	3.16	11.4	30.0^o	27.6^o	3.41

Table 2: Elastic ep calibration kinematic setting.

The results of the calorimeter energy calibration are shown in Fig. 6. The energy resolution for E_e=3.16 GeV was 5.4%. In the second row of Fig. 6, the reconstructed coordinates are plotted. In Fig. 7, a lego plot of calibration coefficients is shown. The calibration coefficients of the blocks located at the edges of the calorimeter have bigger values than those located in the center of the calorimeter.

The energy loss from the side blocks makes the calibration coefficients of those blocks bigger than those of the blocks located in the center of the calorimeter. The

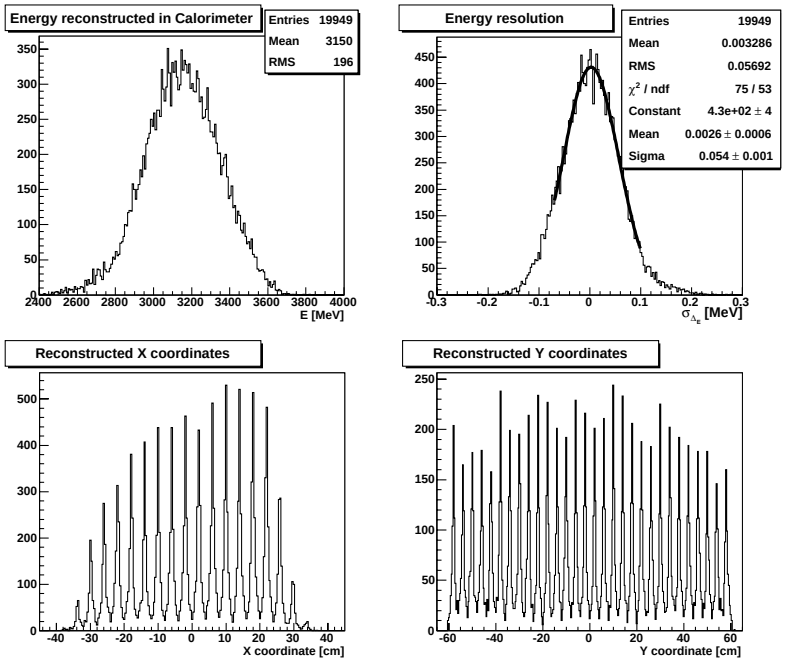

Figure 6: Energy and coordinate reconstruction results. First plot is the reconstructed energy of the particle which initiated an electromagnetic shower in the calorimeter. Second plot is energy resolution in percents. The other two plots are the reconstructed coordinates of the particle.

bigger coefficients compensate for the energy loss from the side blocks. Side blocks of the calorimeter were not used in physics analysis in order to reduce systematic uncertainties.

The influence of the cluster size on the calorimeter's energy resolution was studied as well, see Tb. 3. As it is shown in Tb. 3, the energy resolution for 3×3 cluster is slightly better than that of 5×5 cluster.

Runs	$E(GeV)$	Cluster size	$\frac{\sigma_E}{E}$ (%)	$\frac{\sigma_E}{E}_{E=1GeV}$ (%)	$< C_i >$	$\mathrm{Sig}(C_i)/< C_i >$
1930	3.384	(5×5)	4.5	8.3	0.99	0.062
1930	3.384	(3×3)	4.2	7.7	1.03	0.060
2036-42	4.200	(5×5)	4.5	9.2	1.06	0.077
2036-42	4.200	(3×3)	4.4	9.0	1.03	0.07

Table 3: Calorimeter calibration results for different cluster sizes.

For high beam current with radiator installed (production runs) the level of background was approximately three times higher than that for *ep* elastic runs. Taking

account of this, the production data were analyzed with 3×3 cluster to minimize the contribution of background events.

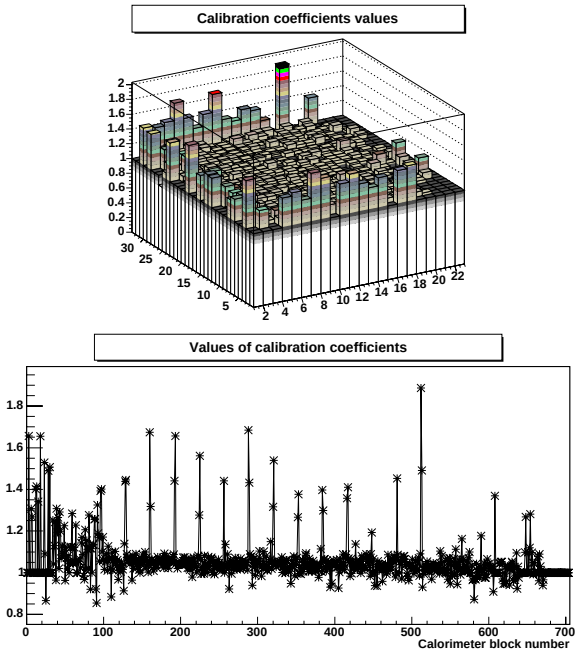

Figure 7: Calorimeter channels calibration coefficient's.

7.3 Stability

Stability of the calorimeter performance is one of the important conditions that should be insured during the data taking period of the experiment.

The performance degradation of the electromagnetic calorimeter is caused by continuous radiation damage to which the calorimeter is subjected during the experiment. The damage causes the reduction of transparency of calorimeter's optical components, in this case the lead glass blocks. The radiation dose that each block receives causes the later to lose its ability to pass Čerenkov light making it less transparent. This causes the Čerenkov light produced in the calorimeter blocks to be absorbed before reaching the cathode of the PMT, leading to the energy resolution loss of the calorimeter. Another reason of energy resolution loss is the non-uniform reduction of each block's transparency. The significant part of the particle's energy is deposited in the first 10-20 cm of the block. The later makes the front part of each block less transparent than the rest of it. This makes the collected light on PMT's cathode highly instable quantity, since it becomes dependent on the position within the block where an electromagnetic shower was initiated. All factors described above contribute to the worsening of the energy resolution.

A study of the calorimeter energy resolution versus total collected beam charge has been performed. The results are shown in Fig. 8. The energy resolution is calculated for 1 GeV according to the following formula:

$$\sigma_E[\%]|_{E=1GeV} = \sigma_E[\%]|_E\sqrt{E[GeV]} \tag{5}$$

As shown in Fig. 8, at the end of the experiment, the energy resolution deteriorated to 11%. It was still enough in order to discriminate the RCS events from the background.

Summarizing, a photon spectrometer was constructed for E99-114 experiment. High energy and angular resolution were the key features of the photon spectrometer. They allowed to estimate the number of RCS events very accurately. The performance of the calorimeter during the experiment was that expected by design.

I thank spokespersons of E99-114 experiment: Charles Hyde-Wright, Alan Nathan and Bogdan Wojtsekhowski for organizing this experiment. I especially thank Armen Ketikyan for being my first teacher and developing the calibration and reconstruction code of the calorimeter. I am grateful to Hakob Voskanyan, Samvel Mayilyan, Albert Shahinyan and Michael Roedelbronn for their work on the calorimeter construction. I thank Kim Egiyan and Kees DeJager for support of my work in Hall A physics program.

This work was supported in part by the National Science Foundation and the US Department of Energy under contract DE-AC05-84ER40150, modification No. M175, under which the Southeastern Universities Research Association (SURA) operates the Thomas Jefferson National Accelerator Facility.

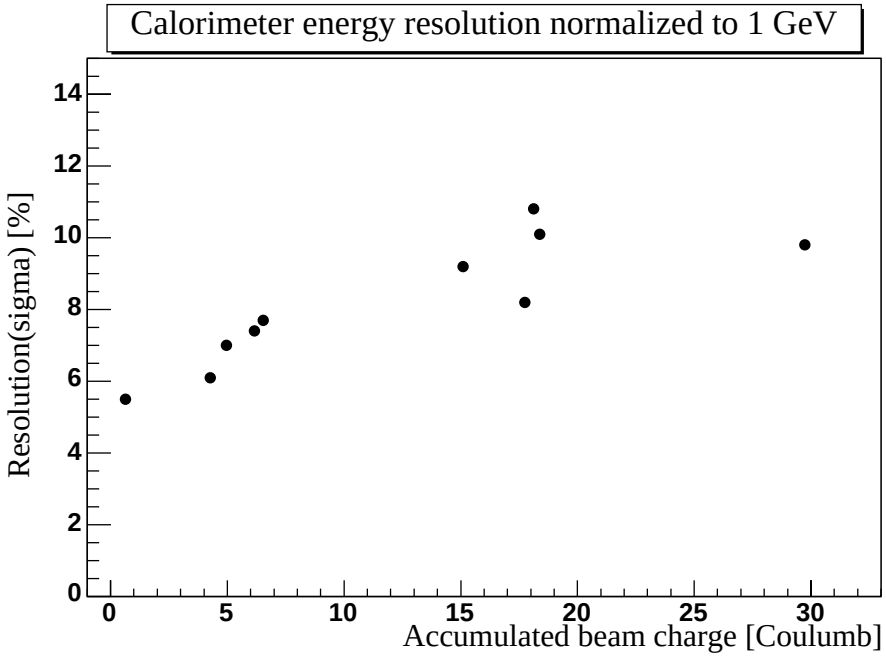

Figure 8: Calorimeter energy resolution degradation.

References

[1] C. Hyde-Wright, A.M. Nathan, and B. Wojtsekhowski (spokespersons), JLab experiment E99-114

[2] M. A. Shupe, et al., *Phys Rev* **D19**, 1929 (1979).

[3] A. Ketikyan et al., E99-114 Study of Hall A Photon Spectrometer, Internal Report, 1999.

[4] Vladimir Popov, Private Communications.